16 February 2001

ELSEVIER

Chemical Physics Letters 335 (2001) 1–8

CHEMICAL PHYSICS LETTERS

www.elsevier.nl/locate/cplett

Production of short carbon nanotubes with open tips by ball milling

N. Pierard [a,*], A. Fonseca [a], Z. Konya [a], I. Willems [a], G. Van Tendeloo [b], J. B.Nagy [a]

[a] *Laboratoire de Résonance Magnétique Nucléaire, FUNDP, 61 rue de Bruxelles, B-5000 Namur, Belgium*
[b] *EMAT, University of Antwerp (RUCA), Groenenborgerlaan 171, B-2020 Antwerp, Belgium*

Abstract

Short multi-wall carbon nanotubes can be obtained by ball milling. The average length of the ball milled carbon nanotubes, synthesised by decomposition of acetylene on different types of supported metal catalysts, is ca. 0.8 μm. The cleavage was caused by the collision between one agate ball and the nanotube powder contained in an agate mortar.

1. Introduction

Since the discovery of nanotubes in 1991 by Iijima [1], this new form of carbon has aroused interest in their fabrication [2] (arc discharge, catalytic decomposition of hydrocarbons, laser ablation...) and also their properties (Young modulus [3], adsorption process [4], electric properties [5–7]). The application fields are various: field emission [8], electric conductivity [9], hydrogen storage [10–13], molecular sieves [14], etc.

As far as the latter two applications are concerned, short nanotubes with open ends are required to overpass the diffusion limitation. Recently, interest has focussed on producing small nanotubes (shorter than 1 μm). The different methods proposed to cut nanotubes are ultrasound power [15–17] and STM voltage [18]. Nevertheless, these techniques are limited to producing milligram scale quantities. Ball milling has already been utilised for production of nanoparticles [19] or nanoporous carbon [20], but also for curving nanotubes [21]. In this paper, we present a new and simple technique to obtain *short nanotubes* in gram scale quantities with open tips by the ball milling process, starting from *long* multi-wall carbon nanotubes. The cleavage was followed by TEM as a function of the ball milling time. A cutting mechanism of the nanotubes based on the collision between one agate ball and the nanotube powder contained in an agate mortar is proposed.

2. Experimental

2.1. Production of the long carbon nanotubes

Multi-wall carbon nanotubes were prepared by catalytic decomposition of acetylene using Co or Co/Fe catalyst supported on NaY zeolite. Catalyst preparation has been already described elsewhere [22–24]. We used the impregnation method with a

* Corresponding author.
E-mail address: nathalie.pierard@fundp.ac.be (N. Pierard).

0009-2614/01/$ - see front matter
PII: S0009-2614(01)00004-5

concentration of 5 wt% for Co alone and 2.5/2.5 wt% for Co/Fe. The production of nanotubes was carried out at 700°C during 1 h using acetylene flow of 30 and 300 ml/min of N_2 as carrier gas. Nanotubes synthesised on Co/NaY and Co/Fe/NaY have an average inner/outer diameter of 6/25 nm (*thick*) and 4/15 nm (*thin*), respectively. Their average length is about 50 μm before the ball milling process.

Nanotube purification was carried out in two steps. First, zeolite and metals were dissolved in concentrated HF (38 wt%) to give nanotubes contaminated by pyrolitic carbon. Secondly, the pyrolitic carbon was eliminated by the $KMnO_4$/H_2SO_4 aq. procedure [24]. 0.2 and 0.3 equivalents of $KMnO_4$ were used in the purification of the *thin* and *thick* nanotubes, respectively.

2.2. Ball milling process

Carbon nanotube powder was introduced in the mortar of the ball milling apparatus containing an agate ball (5 cm in diameter). Ball milling amplitude (vertical vibration intensity) was 3 mm and there were 3000 vibrations/min (Vibration micro-Pulveriser 'Pulverisette 0' Fritsch, 220 V).

Two types of pure nanotubes were studied: *thin* (8.0 g) and *thick* tubes (3.0 g). The same measures were also made on 0.56 g *thin* nanotubes containing pyrolitic carbon.

2.3. Measure of the nanotubes length

The ball milling effect on the nanotubes was analysed by transmission electron microscopy (TEM) (Tecnai 10, Philips). To prepare grids, 1 mg of sample was dispersed in 2 ml of toluene, followed by 2 min sonication. Finally, a drop was deposited on a Cu/Rh grid, covered with formvar, a vinyl polymer, and the grid was dried overnight under vacuum.

2.4. Structural characteristics

Structural characteristics of the nanotubes were observed by TEM and they were also analysed using a powder diffractometer (PW3710 BASED, Philips, Cu K_α radiation: 1.5418 Å).

3. Results and discussion

From TEM observations, it was possible to measure nanotube length and distribution. The evolution of the average nanotube length as a function of the ball milling time was determined for the two types of nanotubes. Structural characteristics of the nanotubes were also studied and a nanotube-cleavage model was elaborated.

3.1. Distribution of carbon nanotubes

TEM observation of the nanotube samples for different ball milling times revealed that the nanotube length decreases with increasing treatment time (Fig. 1). On the untreated nanotubes (Fig. 1a, d), only some tube tips can be seen, most of them belonging to different nanotubes. In fact, the tubes are too long (ca. 50 μm) to fit in a single TEM image. For small treatment periods, TEM observation only allows the emergence of *short nanotubes* (<few micrometers) to be followed. When the grinding time is long enough to make all the nanotubes shorter than 10 μm, the measurement of their length from the TEM pictures (Fig. 1b, c and e, f) becomes easier. On Fig. 2a, b, the nanotube length distributions are shown for different ball milling times. For short treatment times, only the smaller tubes can be measured since the longer tubes form balls and do not fit in a single TEM picture. As a consequence, the long tube lengths cannot be measured by this method. After a few hours of processing, some of the broken nanotubes can be measured (those shorter than 10 μm). This is the reason for the broader distribution. After 10 h of treatment for the *thin* tubes (Fig. 2a) or 16 h treatment for the *thick* ones (Fig. 2b), the nanotube distribution becomes narrow and there are only short nanotubes. It can be stated that during this period all the nanotubes were broken. Further treatment does not affect the *global average length* and no amorphous carbon appears even after 120 h of milling (Fig. 1e, f).

On the high resolution TEM image of *thick* carbon nanotubes after 120 h of milling (Fig. 3), typical short nanotubes with open tips can be seen. On the same picture, the typical nanotube

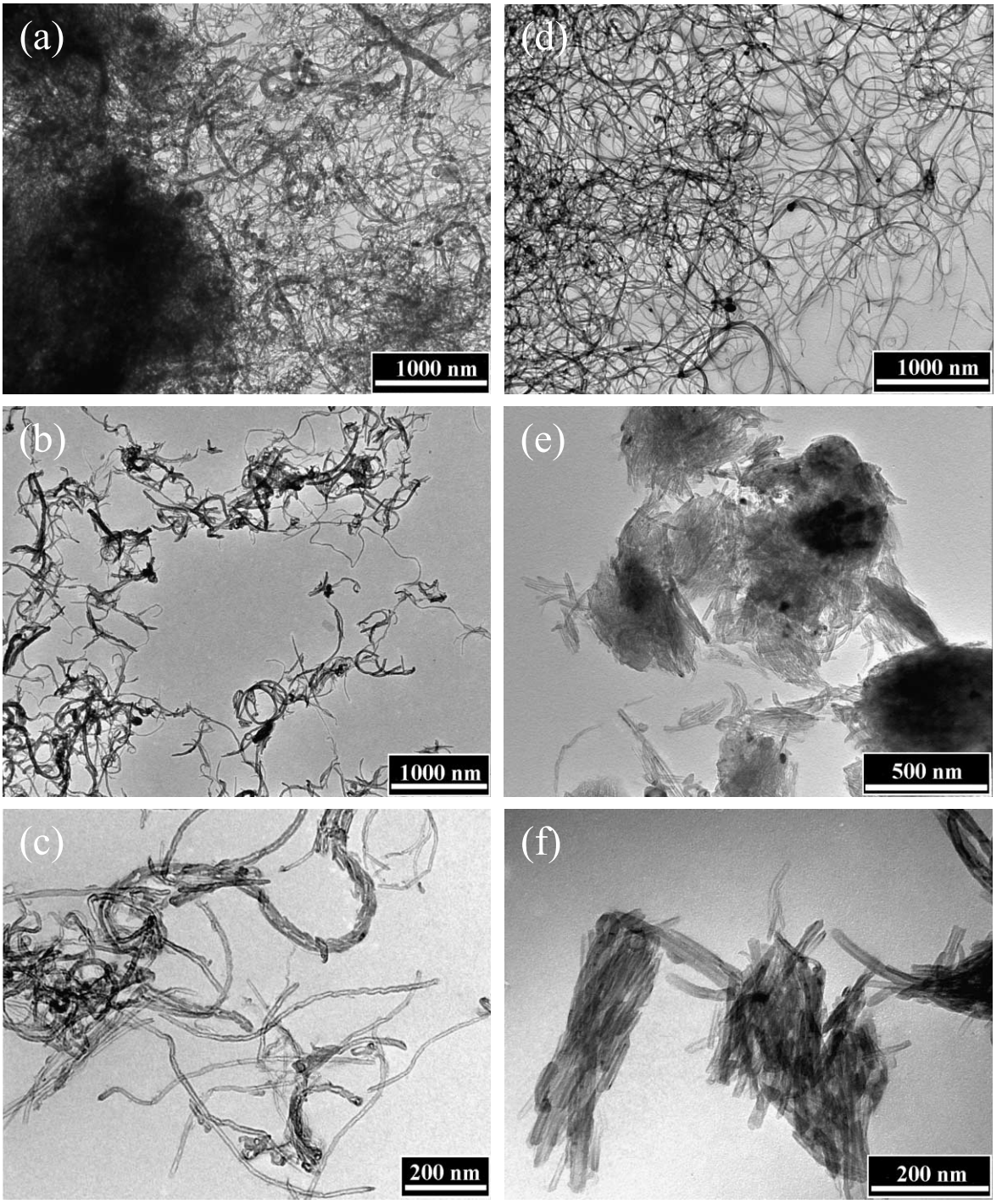

Fig. 1. Low magnification TEM images of multi-wall carbon nanotubes. (a–c) *Thin* nanotubes before (a) and after (b, c) 12 h of ball milling. (d–f) *Thick* nanotubes before (d) and after (e, f) 120 h of ball milling.

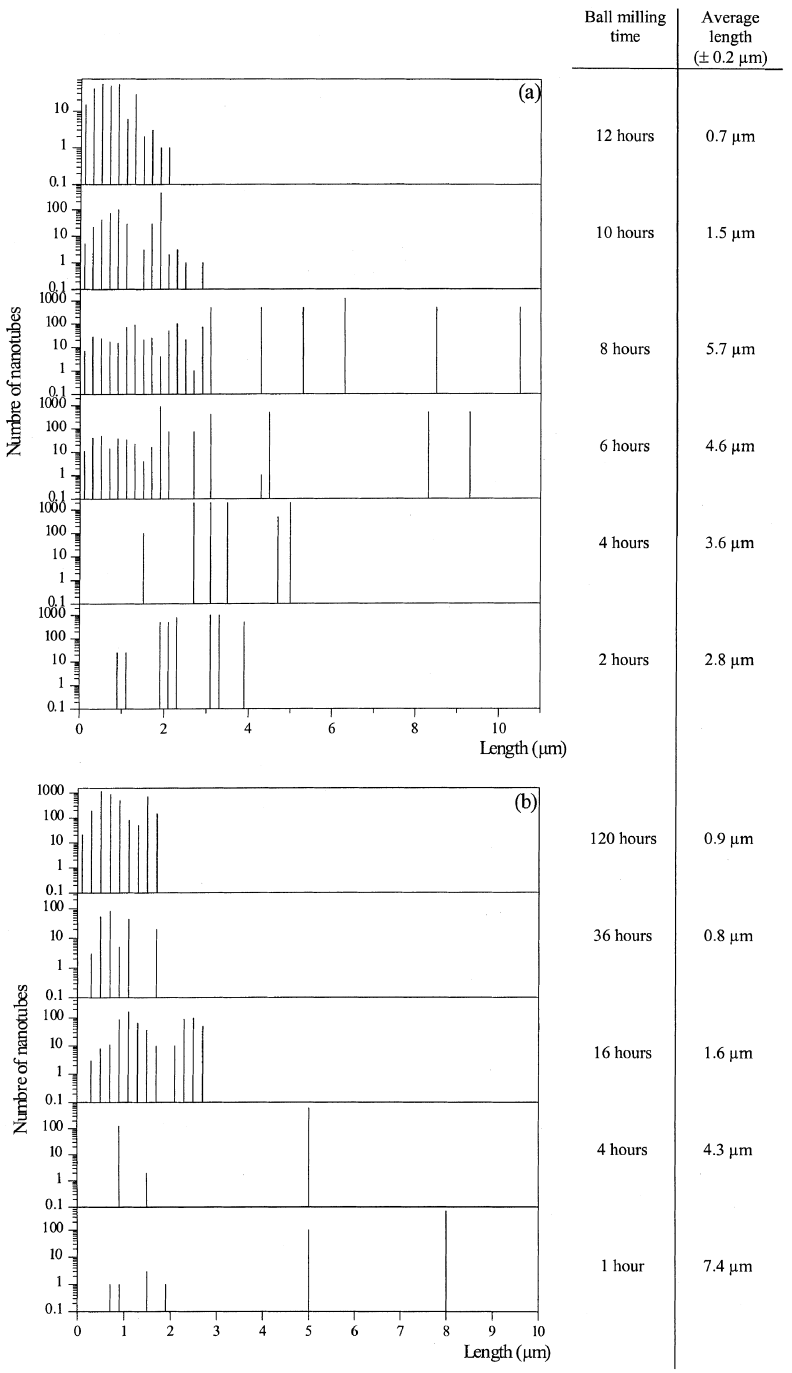

Fig. 2. Measured *thin* (a) or *thick* (b) length distribution of the nanotubes for different ball milling times.

adhesion characteristics of the *thick* nanotubes can also be observed. Note that the adhesion of nanotubes to form bundles (Fig. 1e, f) is only possible for the short nanotubes, because they are all straight. On the mother long nanotubes (Fig. 1a, b), the nanotube adhesion is limited due

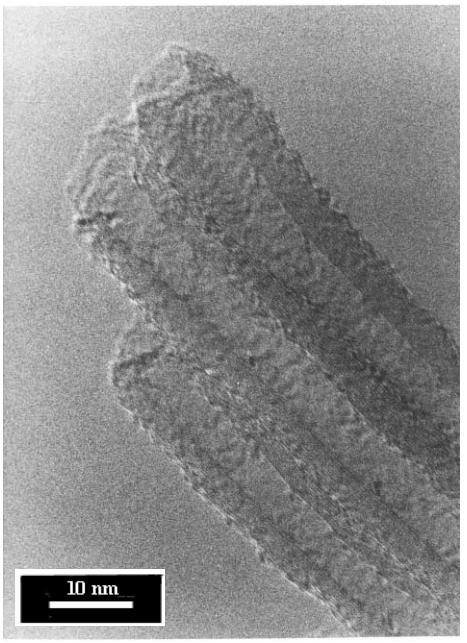

Fig. 3. HREM image of short *thick* carbon nanotubes after 120 h of ball milling.

to the curved shape of the tubes. The higher curvature of the *thin* tubes also limits their adhesion, even when shortened by grinding (Fig. 1a–c). Another interesting observation, comparing the *thin* and *thick* short nanotubes (Fig. 1c, f), is the fact that the *thick* tubes are individual with continuous shape (Fig. 3) while most of the *thin* tubes are composed of several ca. 50–100 nm sections. The latter sections are part of the mother long nanotubes that were partially cleaved by the ball milling effect but were not disconnected (Fig. 1c).

3.2. Time evolution of the average length of carbon nanotubes

The evolution of the average length of the *short nanotubes*, the distribution of which is represented in Fig. 2a, b, is plotted as a function of time in Fig. 4.The curves representing the experimental value for the *short nanotubes* do not include the *long nanotube* distribution because the length of the latter cannot be measured on a single TEM picture. For that reason, other curves are added to the graphs to represent disappearance of the *long nanotubes* with increasing ball-milling time. The weighted mean of the lengths of *long* and *short* nanotubes gives the length evolution of the *global nanotubes* (Fig. 4). The latter evolution as a function of the grinding time can be approximated by the following converging decreasing exponential:

$$\textit{Global nanotubes}\ \text{length}\ (\mu\text{m}) = A + \left[50\left(1 - \frac{t}{P+t}\right) + 10\left(\frac{t}{P+t}\right)\right] \mathrm{e}^{-(\ln 2/P)t},$$

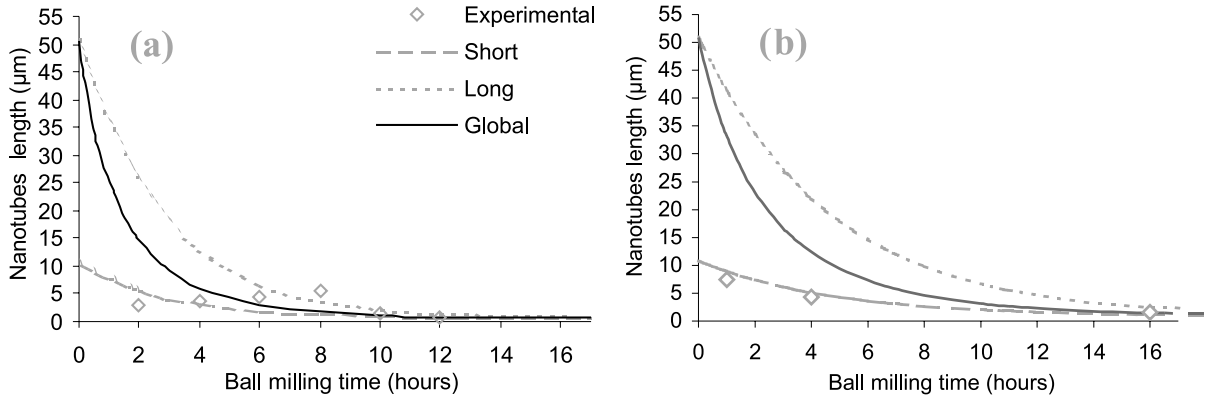

Fig. 4. Time evolution of carbon nanotube average length for *thin* (a) and *thick* (b) nanotubes.

where t is the grinding time (h), $A = 0.7$ or 0.9 μm for *thin* or *thick* nanotubes, respectively, P is the period of the *short* nanotube length evolution = 2 or 3 h for *thin* or *thick* nanotubes, respectively.

The periods, 2 h for the *thin* tubes and 3 h for the *thick* ones, are characteristics of their resistance to the ball milling efficiency. The thinner the nanotubes, the faster they cleave. The length A (0.7 μm for *thin* tubes and 0.9 μm for *thick* tubes) depends on the thickness of the original nanotubes. According to the equation, after five periods of cleavage, the average length of the *global nanotubes* reaches its final value of A, within 3%. The further tumbling of the nanotubes, up to 120 h (Fig. 2b) does not change the final length of the nanotubes. Moreover, it is important to note that no other forms of carbon but nanotubes are observed, even after 120 h of grinding.

3.3. Structural characteristics

3.3.1. TEM

After 10 h for *thin* tubes or 15 h for the *thick* ones, the samples are homogeneous. It means that all nanotubes are broken and no *long nanotubes* remain. The high-resolution TEM image (Fig. 3) clearly shows that the nanotube structure is not damaged and that the tubes have open tips. This last feature is very important for the applications that will take advantage of the possible confinement effect in the nanotube cavity such as gas adsorption and separation or confinement limited reactions.

Since the nanotubes cleaved in this paper were previously treated by HF and also by $KMnO_4$, the nanotube length convergence to ca. 0.8 μm may depend on their structural characteristics. In fact, the two treatments oxidise the nanotubes and introduce oxygenated functions (COOH,...) at the end of the tubes and at the structural defects. After the oxidation treatment, the nanotubes are dried and the inter-tube dehydration can cross-link the nanotubes. The resulting material is reticulated and more rigid. As a result, the ball's collision could be more efficient. For the sake of knowing if the efficiency of the ball milling process is linked to the presence of functional groups on the outer surface of the nanotubes, other nanotube samples were also cleaved by ball milling. It was observed that the ball-milling crack for 16 h of a crude *thin* nanotube sample (after HF treatment only) gives short nanotubes of 1.0 μm average length. The latter result excludes the necessity of oxidation treatment on the nanotubes before grinding, but the efficiency of the ball mill cutting is lower. Other crude multi-wall nanotube samples produced by

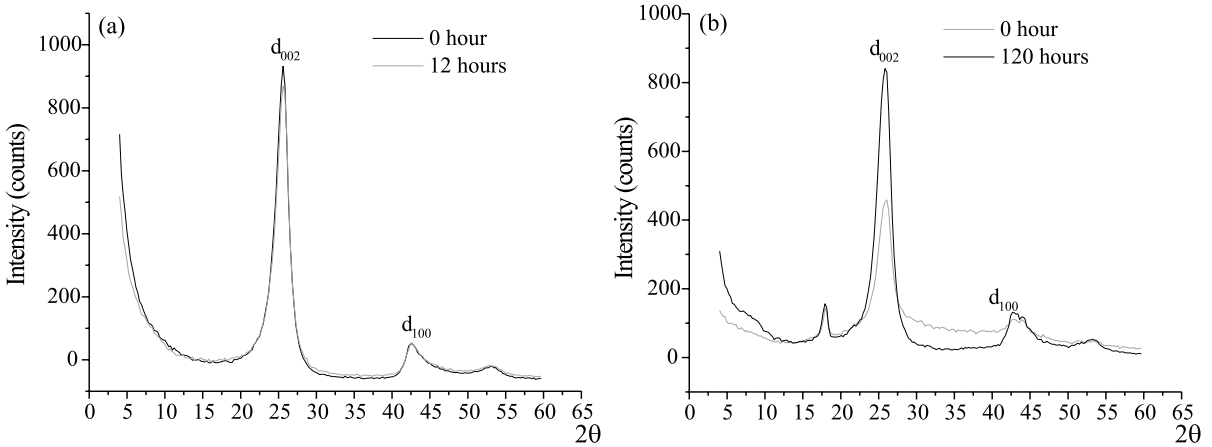

Fig. 5. Powder X-ray diffractograms before and after grinding for *thin* (a) and *thick* (b) nanotubes.

CVD, containing the catalyst and the support, were also successfully cleaved applying the same ball milling process.

3.3.2. Powder XRD

Fig. 5a, b shows the XRD patterns of *thin* and *thick* nanotubes before and after 12 h and 120 h of treatment, respectively. The similarity of the positions of the d_{002} and d_{100} peaks for the MWNTs shows that the graphitization remains almost the same for both samples. It confirms that the fracture is very localised, as already observed by TEM.

3.3.3. Nanotube cleavage mechanism

First, the nanotube cleavage is easier at the place of structural defects such as the curvatures. In fact, when the tubes are curved, they are made by continuous or partly discontinuous junctions of straight nanotubes. The latter junctions are nanotube defects where they can break by compression.

Secondly, when a straight or slightly curved nanotube is compressed, it is not broken. The crushing is reversible if the nanotube end is moving free and absorbs elastically the mechanical constraints. On the other hand, if the nanotube is held in a matrix, such as cross-linked nanotubes after dehydration, it breaks because it cannot absorb elastically the mechanical constraints.

4. Conclusions

The ball milling process is a good method to obtain *short* (<1 μm) multi-wall carbon nanotubes with open tips. The cleavage of catalytically synthesised multi-wall carbon nanotubes (either crude or purified) gives *short nanotubes*. The average length varies from 0.7 to 0.9 μm. Moreover, homogeneous nanotube samples are obtained and no other form of carbon is generated during ball milling (even after 120 h of processing). The nanotube final length depends mainly on the characteristics of the ball milling apparatus, while the resistance of the nanotubes to cleavage depends on their diameter.

Acknowledgements

N. Pierard and I. Willems gratefully acknowledge support from FRIA. The authors thank the Belgian Programme on Inter University Poles of Attraction initiated by the Belgian State, Prime Minister's Office for Scientific, Technical and Cultural Affairs (OSTC-PAI-IUAP No. 4/10 on Reduced Dimensionality Systems) for financial support.

References

[1] S. Iijima, Nature 354 (1991) 56.
[2] C. Journet, P. Bernier, Appl. Phys. A 67 (1998) 1.
[3] M.M.J. Treacy, T.W. Ebessen, J.M. Gibson, Nature 381 (1996) 678.
[4] M.S. Dresselhaus, K.A. Williams, P.C. Eklund, MRS Bull. 24 (11) (1999) 45.
[5] T.W. Ebbessen, Ann. Rev. Mater. Sci. 24 (1994) 235.
[6] J.W. Mintmire, B.D. Dunlap, C.T. White, Phys. Rev. Lett. 68 (1992) 631.
[7] K. Harigaya, Phys. Rev. B 45 (1992) 12071.
[8] W. Zhu, C. Bower, O. Zhou, G. Kochanski, S. Jin, Appl. Phys. Lett. 75 (6) (1999) 873.
[9] C. Dekker, Physics Today (1999) 22.
[10] C. Dillon, K.M. Jones, T.A. Bekkedahl, C.H. Hiang, D.S. Bethune, M.J. Heben, Nature 386 (1999) 377.
[11] C. Liu, Y.Y. Fan, M. Liu, H.T. Cong, H.M. Cheng, M.S. Dresselhaus, Science 286 (1999) 1127.
[12] Y. Ye, C.C. Ahn, C. Witham, B. Fultz, J. Liu, G. Rinzler, D. Colbert, K.A. Smith, R.E. Smalley, Appl. Phys. Lett. 74 (16) (1999) 2307.
[13] P. Chen, X. Wu, J. Lin, K.L. Tan, Science 285 (1999) 91.
[14] Q. Wang, S.R. Challo, D.S. Sholl, J.K. Johnson, Phys. Rev. Lett. 82 (5) (1999) 956.
[15] K.L. Lu, R.M. Lago, Y.K. Chen, M.L.H. Green, P.J.F. Harris, S.C. Tsang, Carbon 34 (1996) 814.
[16] K.B. Shelimov, R.O. Esenaliev, A.G. Rinzler, C.B. Huffman, R.E. Smalley, Chem. Phys. Lett. 282 (1998) 429.
[17] J. Liu, A.G. Rinzler, H. Dai, J.H. Hafner, R.K. Bradley, P.J. Boul, A. Lu, T. Iverson, K. Shelimov, C.B. Huffman, F. Rodriguez-Macias, Y.-S. Shon, T.R. Lee, D.T. Colbert, R.E. Smalley, Science 280 (1998) 1253.
[18] L.C. Venema, J.W.G. Wildöer, H.L.T. Twinsta, C. Dekker, A.G. Rinzler, R.E. Smalley, Appl. Phys. Lett. 71 (18) (1999) 2629.
[19] Y.B. Li, B.Q. Wei, J. Liang, Q. Yu, D.H. Wu, Carbon 37 (1999) 493.
[20] Y. Chen, J.F. Gerald, L.T. Chadderton, L. Chaffron, Appl. Phys. Lett. 74 (19) (1999) 2782.

[21] J.Y. Huang, H. Yasuda, H. Mori, Chem. Phys. Lett. 303 (1999) 130.
[22] P. Piedigrosso, Z. Konya, J.-F. Colomer, A. Fonseca, G. Van Tendeloo, J. B.Nagy, Phys. Chem. Chem. Phys. 2 (2000) 163.
[23] I. Willems, Z. Konya, J.-F. Colomer, G. Van Tendeloo, N. Nagaraju, A. Fonseca, J. B.Nagy, Chem. Phys. Lett. 371 (2000) 71.
[24] K. Hernadi, A. Fonseca, J. B.Nagy, D. Bernaerts, A. Fudala, A.A. Lucas, Zeolites 17 (1996) 416.